



# Anticorrosive properties of polypyrrole films modified with zinc onto SAE 4140 steel



I.L. Lehr, S.B. Saidman\*

Instituto de Ingeniería Electroquímica y Corrosión (INIEC), Departamento de Ingeniería Química, Universidad Nacional del Sur, Av. Alem 1253, 8000 Bahía Blanca, Argentina

## ARTICLE INFO

### Article history:

Received 9 October 2012

Received in revised form 27 June 2013

Accepted 6 July 2013

Available online 31 July 2013

### Keywords:

Polypyrrole

Zinc

AOT

Anticorrosive properties

SAE 4140 steel

## ABSTRACT

Polypyrrole (PPy) films modified with zinc were electrosynthesized onto SAE 4140 steel in presence of bis(2-ethylhexyl) sulfosuccinate (AOT). The Zn and PPy electrodeposition was realized by using cyclic voltammetry at different temperatures. The corrosion protection properties of the films were examined in chloride solution by open circuit measurements, linear polarization and electrochemical impedance spectroscopy (EIS). The obtained results indicate that the presence of Zn in the polymer matrix improves the anticorrosive performance of PPy films. The best anticorrosion efficiency was obtained for the coatings modified at 20 °C which provided anodic protection to the steel substrate for a long period of immersion in chloride solution. Cathodic protection was observed when the electrodeposition temperature was increased. Adherence and anticorrosive properties declined sharply for the coatings electrosynthesized at 5 °C.

© 2013 Elsevier B.V. All rights reserved.

## 1. Introduction

Conducting polymers have been studied during the last decades due to their diverse applications such as corrosion protection coatings [1,2]. These polymers have emerged as a good alternative to coatings that contain heavy metals or other environmentally problematic materials such as hexavalent chromium. The most studied conducting polymers are polypyrrole (PPy) and polyaniline (PANI) deposited on oxidizable substrates [3]. Both, structural and electronic properties of conducting polymers, which depend on the synthesis conditions, determine the degree of corrosion protection of the coatings [4].

The practical applications of conducting polymers coatings are complicated because the protection time and the anticorrosive efficiency of the films are limited. In this aspect, one of the main problems is the presence of porosity in the coating. Water uptake process occurs along these pores and, accordingly the formation of ionically conducting paths takes place between the corrosive environment and the substrate surface. As the immersion time elapses, this process produces a decrease in the degree of corrosion protection. The modification of polymer coatings by application of metallic electrodeposits or some top coatings is a possibility to improve the anticorrosive performance [3]. In this regard, the modification of conducting polymers films with noble

metals increases the anticorrosive properties due to stabilization of the metal potential within the passive region for more prolonged time. Another alternative is the incorporation of active metals in the conducting polymer matrix. Among them Zn is one of the most investigated. This metal is widely used to protect steel surfaces because Zn coatings have excellent adhesion and resistance for abrasion and corrosion. Zn is preferentially oxidized, covering the substrate with a passive hydroxide–oxide film. Several works have reported an increment of the anticorrosive properties of conducting polymers films by Zn incorporation in the polymeric matrix [5–10]. Tüken et al. [10,11] reported an improvement in the anticorrosive properties by the electrodeposition of Zn onto PPy and PANI coatings, which are previously electroformed onto mild steel. The presence of Zn and its corrosion products reduces the permeability of films and provides cathodic protection to mild steel. In other report, Herrasti et al. [12] informed that the electrodeposition of Zn microparticles on previously deposited polymer layers promotes a decrease in the corrosion current in highly aggressive solutions and that Zn acts as an anodic corrosion inhibitor.

On the other hand, the presence of surfactants in the electrodeposition solution improves the efficiency of the process and also modifies the deposits morphology. Previous works have shown that the electrosynthesis of PPy in AOT-containing solutions onto Al [13], Fe [14] and Ti [15] allows obtaining films with good anticorrosive properties. In all these cases, the AOT molecule plays the dual role of dopant and surfactant. On the other hand, we have reported that the Zn nucleation-growth process and consequently the

\* Corresponding author. Tel.: +54 291 4595182; fax: +54 291 4595182.  
E-mail address: [ssaidman@criba.edu.ar](mailto:ssaidman@criba.edu.ar) (S.B. Saidman).

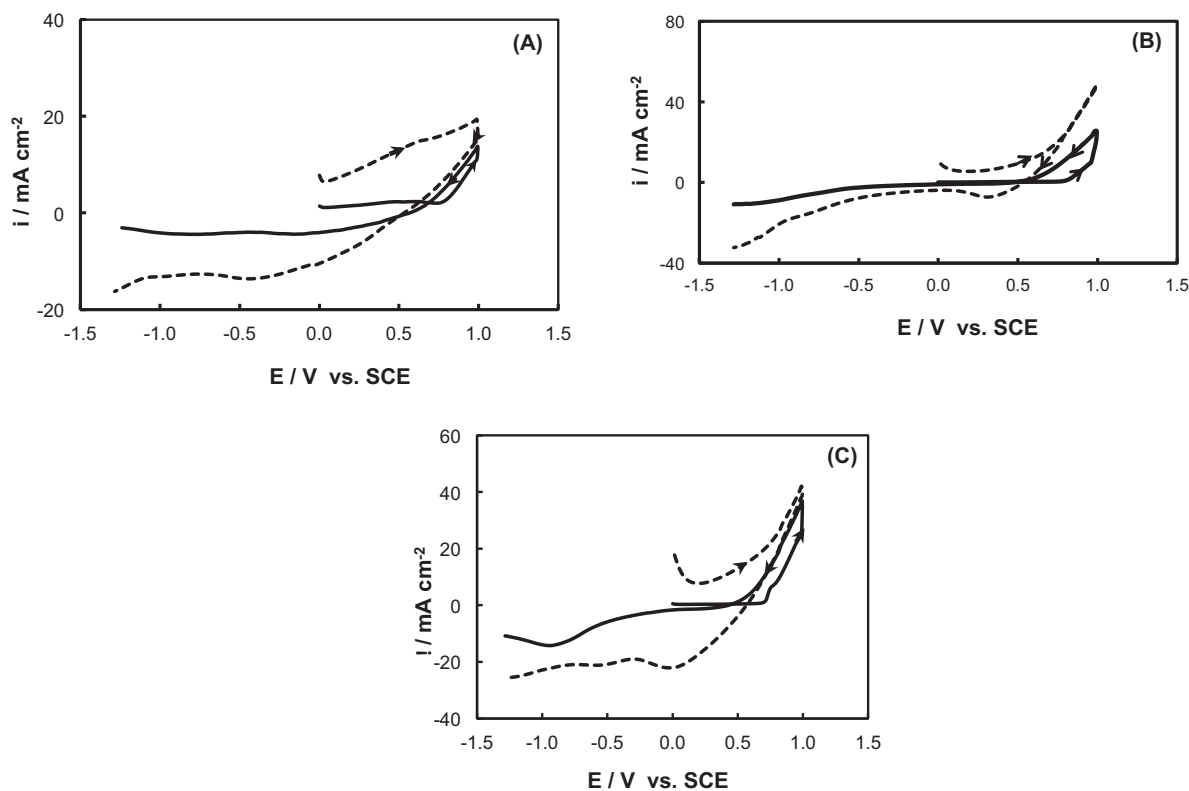


**Fig. 1.** Triangular potential sweep for SAE 4140 steel electrode at  $0.05 \text{ V s}^{-1}$  in  $0.05 \text{ M AOT} + 0.05 \text{ M ZnSO}_4 + 0.1 \text{ M Py}$  at (A)  $5^\circ\text{C}$ , (B)  $20^\circ\text{C}$  and (C)  $40^\circ\text{C}$ . Initial potential:  $0.0 \text{ V}$ . Starting in an anodic direction until reaching a value of  $1.0 \text{ V}$  (timeout of  $90 \text{ s}$ ). The cathodic limit was set in  $-1.30 \text{ V}$ . Scans 1 (full line) and 10 (discontinuous line) are displayed.

morphology of the electrodeposits were modified in the presence of AOT inducing the formation of a porous coating [16].

In this paper, we present results on the electrodeposition of PPy coating modified with Zn onto SAE 4140 steel in solutions containing AOT. The objective was to analyze the behavior of Zn in the anticorrosive performance of PPy films. The effects of electrosynthesis parameters such as the electrochemical technique employed and electrodeposition temperature on the morphology and anticorrosive properties were studied. The characterization of the films was done using electrochemical techniques and SEM/EDX. For comparative purposes, the anticorrosive behavior was also checked for unmodified PPy films and uncoated SAE 4140 steel.

## 2. Experimental

### 2.1. Chemicals and materials

All chemicals were reagent grade and solutions were made with twice distilled water. Pyrrole was purchased from Across Organics and it was freshly distilled under reduced pressure before use. In order to avoid the slow hydrolysis of AOT all the measurements were done with freshly prepared samples.

SAE 4140 steel rods embedded in a Teflon holder with an exposed area of  $0.070 \text{ cm}^2$  were used as working electrodes. The auxiliary electrode was a large Pt sheet and a saturated calomel electrode (SCE) was used as a reference electrode.

### 2.2. Instrumentation

The cell was a  $20 \text{ cm}^3$  Metrohm measuring cell. Electrochemical measurements were done using a potentiostat–galvanostat PAR 273A and VoltaLab40 Potentiostat PGZ301. The frequency used

for the impedance measurements was changed from  $100 \text{ kHz}$  to  $10 \text{ mHz}$  and the signal amplitude was  $10 \text{ mV}$ .

A dual stage ISI DS 130 SEM and an EDAX 9600 quantitative energy dispersive X-ray analyzer were used to examine the electrode surface characteristics.

Electrical conductivity was measured by two-probe method using a homemade device and film adhesion was tested using 3M scotch tape.

The elemental analysis was carried out with an atomic emission spectrometer with inductively coupled plasma (ICP-AES), Shimadzu's simultaneous ECPE-9000, according to EPA 200.7 method.

### 2.3. Electrosynthesis and characterization of coatings

Electropolymerization was performed in solutions containing  $0.05 \text{ M AOT}$ ,  $0.05 \text{ M ZnSO}_4$  and  $0.1 \text{ M pyrrole (Py)}$  in a purified nitrogen gas saturated atmosphere. Before each experiment, the exposed surfaces were polished to a  $1000 \text{ grit}$  finish using SiC, then degreased with acetone and washed with triply distilled water.

The corrosion performance was investigated in  $0.5 \text{ M NaCl}$  solution by a potentiodynamic method, the variation of the open circuit potential (OCP) as a function of time and electrochemical impedance spectroscopy. The variation of the open circuit potential (OCP) as a function of time can be used to evaluate the degree of corrosion protection attained after covering the substrate with the conducting polymer.

The Tafel tests were carried out by polarizing from cathodic to anodic potentials with respect to the open circuit potential at  $0.001 \text{ V s}^{-1}$  in aerated  $0.5 \text{ M NaCl}$  solution. Estimation of corrosion parameters were realized by the Tafel extrapolation method. The extrapolation of anodic and/or cathodic lines for charge transfer controlled reactions gives the corrosion current density ( $i_{\text{corr}}$ ) at the corrosion potential ( $E_{\text{corr}}$ ). All experiments were conducted after

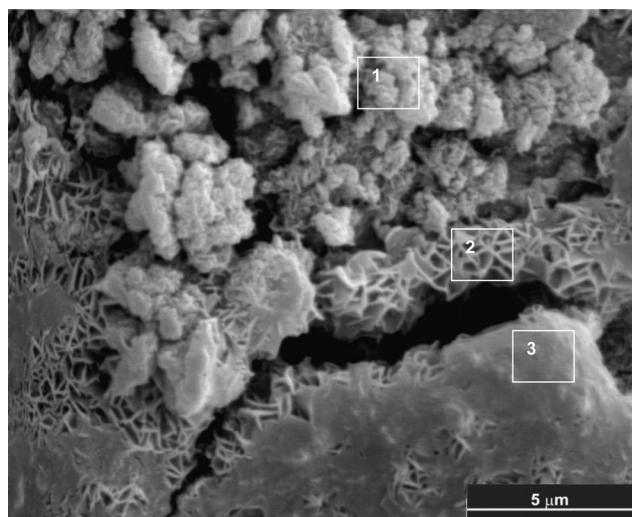


Fig. 2. SEM micrograph of SAE/PPy-Zn(20 °C).

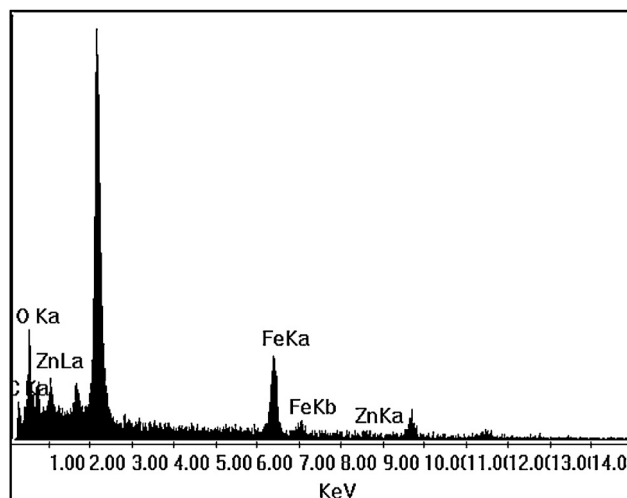


Fig. 3. EDX spectrum of SAE/PPy-Zn(20 °C).

the steady-state  $E_{\text{corr}}$  was attained, which normally took 1 h after immersion in the solution.

The electrodes were allowed to equilibrate at the fixed voltage before the ac measurements.

### 3. Results and discussion

#### 3.1. Electrochemical synthesis

The coatings were electrodeposited in a solution containing 0.05 M AOT, 0.05 M  $\text{ZnSO}_4$  and 0.1 M Py. After preliminary experimentations, a repetitive triangular potential sweep at  $0.050 \text{ V s}^{-1}$  with potential holding at the anodic switching potential was found to be the optimum method for obtaining adherent and homogeneous coatings. Fig. 1 shows the resultant voltammograms obtained starting in an anodic direction from 0.0 V to 1.0 V (timeout of 90 s) and then the cathodic limit was set in  $-1.30 \text{ V}$  at three different temperatures. When the potential is scanned from 0.0 V to the anodic region the current increases at 0.6 V due to pyrrole oxidation and subsequent polymerization. When the potential is reversed, after the polymerization step the current remains low until a new increase in current is seen at  $-0.5 \text{ V}$  which is principally associated with Zn electrodeposition. It was found that 10 cycles produced the best condition for coating growth.

Strongly adherent films were formed at 20 °C (PPy-Zn(20 °C)) and 40 °C (PPy-Zn(40 °C)), while poor adhesion was observed for the polymer grown at 5 °C (PPy-Zn(5 °C)).

The coatings were also synthesized under potentiostatic polarization. The electrode was first polarized to 1.0 V after which a polarization at  $-1.3 \text{ V}$  was applied. The obtained films were easily removed from the substrate, independently of the electrosynthesis temperature and polarization times.

PPy films were also electrosynthesized in the absence of AOT. A solution containing 0.05 M  $\text{Na}_2\text{SO}_4$ , 0.05 M  $\text{ZnSO}_4$  and 0.1 M Py was used for the electropolymerization. The total charge involved in the electroformation of the coating (voltammogram not presented here) is lower than for the polymer electrosynthesized in the presence of the surfactant, indicating that the process is more difficult.

#### 3.2. Morphology of PPy films

The SEM images of the sample PPy-Zn(20 °C) are shown in Fig. 2. The coating presents the typical granular morphology. Labyrinthine

structures can be also observed which are identical to those corresponding to Zn electrodeposits prepared from AOT [16] and also from an ethylene glycol solution of zinc acetate [17]. Some zones are covered with a smooth material probably constituted by  $\text{Zn}(\text{AOT})_2$ . The EDX spectrum in square 2 presents the signal of Zn (Fig. 3). The images from EDX mapping of sample SAE/PPy-Zn(20 °C) electrodeposited after 5 potential scans are shown in Fig. 4. The S image is approximately the inverse to the Zn image.

EDX was also utilized to check the semi-quantitative chemical composition of the coating shown in Fig. 4. The average composition (atomic percentages) determined by SEM/EDX for this film (PPy-Zn<sub>5</sub>) is presented in Table 1. The results obtained for the coating synthesized after 10 potentiodynamic cycles (PPy-Zn<sub>10</sub>) are also included in the same table. The elements C, O, Zn, S and Fe were analyzed. The S signal is obviously associated with the AOT which is the polymer dopant. The Zn:S atomic ratio increases significantly with the number of potential scans, being 0.528 for 5 cycles and 2.259 for 10 cycles. The relative amount of zinc in the coating increases with the number of cycles while the relative amount of polymer diminishes. Moreover, the Fe signal decreases with increasing thickness of the coating, as expected.

When the experimental temperature for deposition was elevated to 40 °C only the deposition of the usual granular structure occurred (Fig. 5). There is no signal of Zn in the EDX spectrum. However, the analysis of a cross-sectional area of the coating obtained after a transverse cut surface near the steel shows a content of Zn. Thus, the distribution of Zn in the polymer is not uniform.

When the electropolymerization was done in the absence of Zn ions (PPy(20 °C)) a coating with a very porous structure was obtained instead of a continuous film (Fig. 6). On the other hand, the polymer obtained in the absence of AOT shows a labyrinthine structure of Zn and less amount of the polymer (image not presented here) compared to the coating electrodeposited in presence of the surfactant.

Table 1

Average composition (atomic percentages) determined by EDX for PPy films modified with Zn at 20 °C obtained after 5 (PPy-Zn<sub>5</sub>) and 10 cycles (PPy-Zn<sub>10</sub>).

Sample (at%)	C	O	Zn	S	Fe	Sum
PPy-Zn <sub>5</sub>	22.632	54.471	4.411	8.412	8.074	100
PPy-Zn <sub>10</sub>	21.663	60.625	10.935	4.84	1.937	100

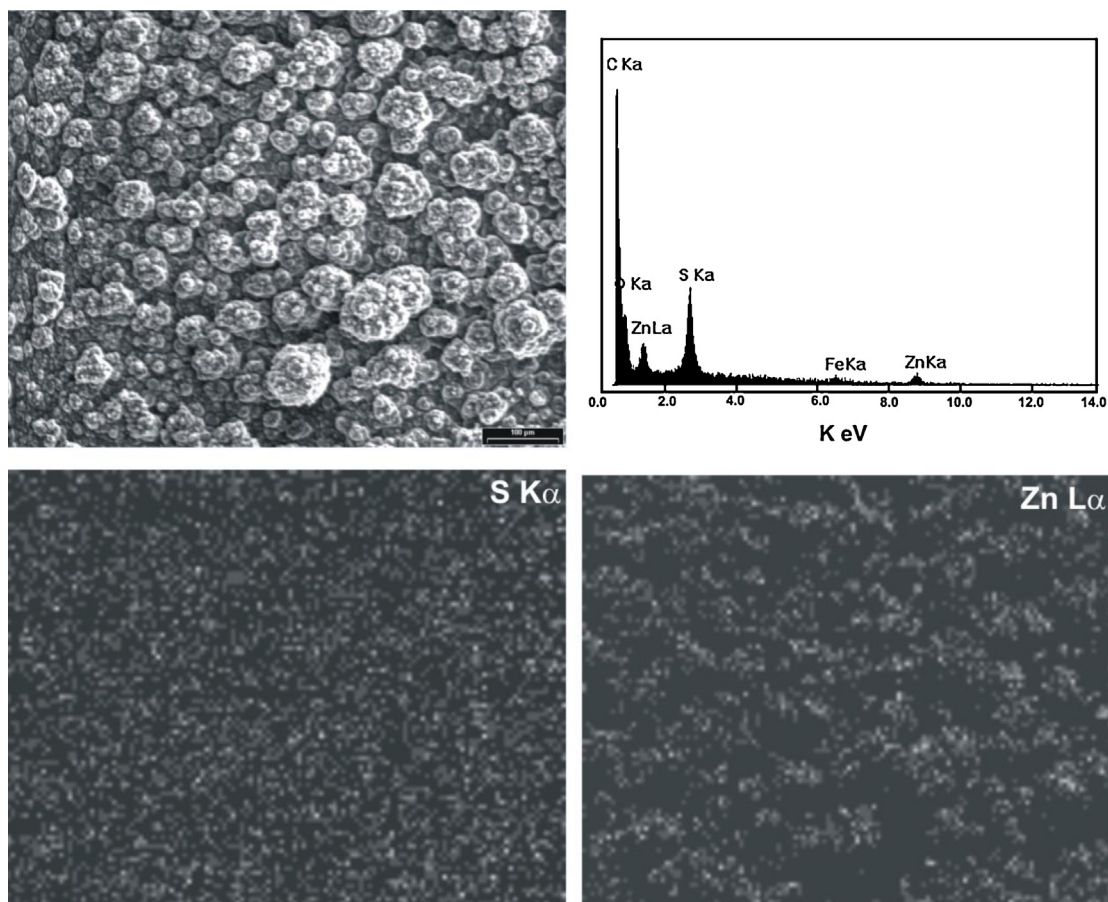


Fig. 4. EDX mapping of SAE/PPy-Zn(20 °C). The coating was obtained after five potential scans in the electrodeposition solution.

### 3.3. Anticorrosion behavior

The variation of corrosion potential ( $E_{\text{corr}}$ ) with time was recorded in 0.5 M NaCl for the steel covered by the films. The OCP of the bare sample was  $-0.57$  V and did not change significantly with increasing exposure time. The potential of the film formed in a solution without the presence of Zn shifts toward less negative values in the first stage of immersion and then shows a constant value of  $-0.11$  V (Fig. 7A). Since this potential is higher than that of the uncoated steel it can be considered that the substrate is protected

during this period. But after 3 h the potential drops to the  $E_{\text{corr}}$  of the bare steel. For the coating electro synthesized in the absence of AOT, the initial potential was  $-0.29$  V and then decreased markedly until it reached the corrosion potential value for uncoated SAE 4140 steel after two hours of immersion (Fig. 7B). A different behavior was registered for the PPy-Zn(20 °C). In spite of the fact that the OCP moves smoothly in the negative direction, it is maintained in the range of the redox potential of PPy even after 30 days of immersion (Fig. 7C).

The initial OCP values measured for the steel electrode covered by PPy-Zn(40 °C) are very negative indicating that a cathodic protection operates. A shift toward more positive potentials begins

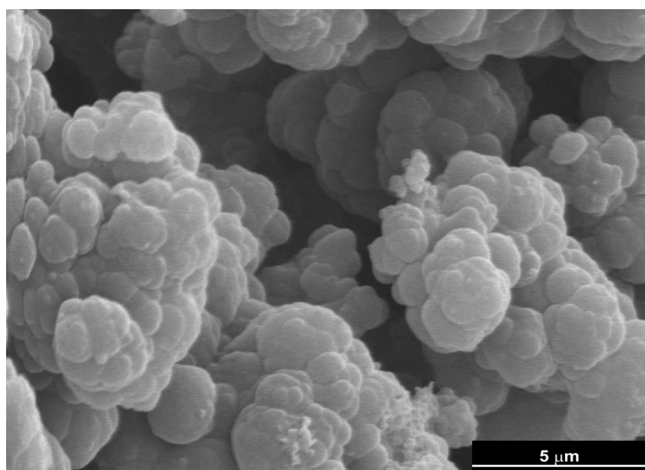


Fig. 5. SEM micrograph of SAE/PPy-Zn(40 °C).

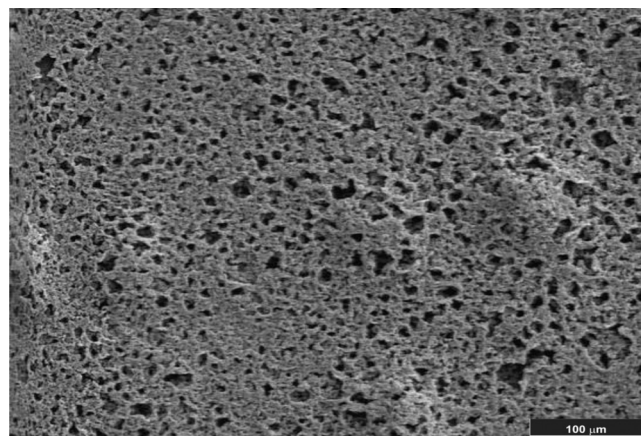
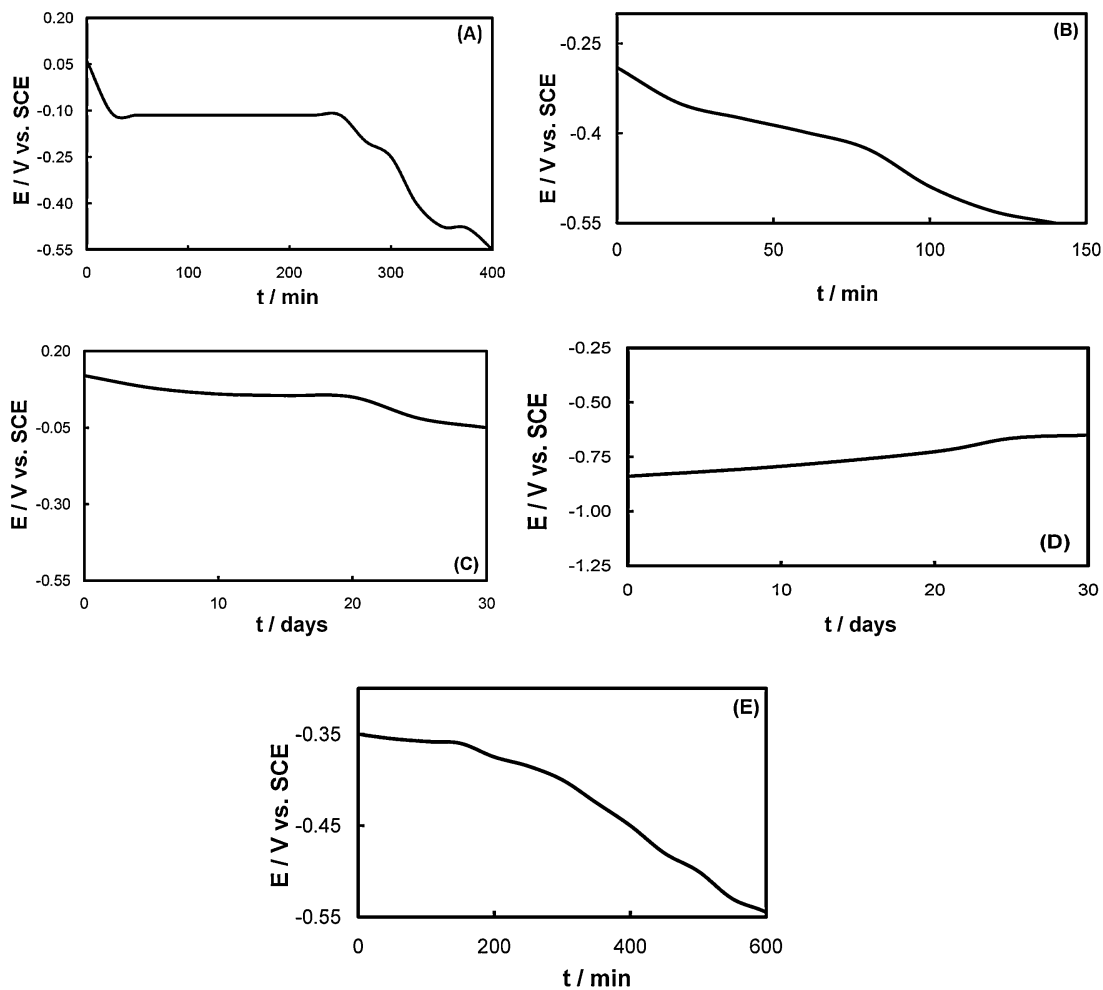


Fig. 6. SEM micrograph of PPy(20 °C).



**Fig. 7.** Time dependence of the OCP in 0.5 M NaCl for (A) SAE/PPy(20 °C), (B) SAE/PPy-Zn obtained in the absence of AOT, (C) SAE/PPy-Zn(20 °C), (D) SAE/PPy-Zn(40 °C) and (E) SAE/PPy-Zn(5 °C).

almost immediately upon immersion in chloride solution, and the potential practically reaches the OCP of the bare substrate after 30 days of exposure (Fig. 7D). The initial OCP value for PPy-Zn(5 °C) was  $-0.35$  V, where it remained for 2 h (Fig. 7E). After this period, the OCP drops to a value corresponding to the corrosion potential for the uncoated steel. Thus, the degree of protection attained is low.

It can be concluded from the OCP measurements that the best protection for the steel was achieved with PPy-Zn(20 °C). Moreover this coated electrode was examined after 30 days of exposure to the corrosive medium (Fig. 8). The absence of any detectable change in the polymer surface indicates no occurrence of substrate corrosion.

The corrosion performance of the samples was also analyzed by comparing the Fe quantity released under OCP conditions in 0.5 M NaCl solution during 30 days of immersion (Table 2). In the case of the bare substrate the immersion time was shorter (96 h).

**Table 2**

Elemental analysis corresponding to a 0.5 M NaCl solution after a sample was immersed: uncoated SAE 4140 steel after 4 days of immersion; PPy-Zn(20 °C) coated SAE 4140 steel and PPy-Zn(40 °C) coated SAE 4140 steel, both after 30 days of immersion.

Sample/immersion time	Fe (mg/L)	Zn (mg/L)	S (mg/L)
SAE/PPy-Zn(40 °C)/30 days	$0.74 \pm 0.02$	$2.11 \pm 0.06$	$1.78 \pm 0.07$
SAE/PPy-Zn(20 °C)/30 days	$0.011 \pm 0.002$	$10.4 \pm 0.2$	$12.8 \pm 0.3$
Uncoated SAE 4140 steel/4 days	$4.6 \pm 0.2$	–	–

The quantity released of Fe is low when the coating was formed at 40 °C but this quantity was reduced significantly for the film synthesized at 20 °C, confirming its excellent performance even after a long exposure time. On the other hand, the concentrations of Zn and S in solution were also analyzed. The obtained results corrobo-

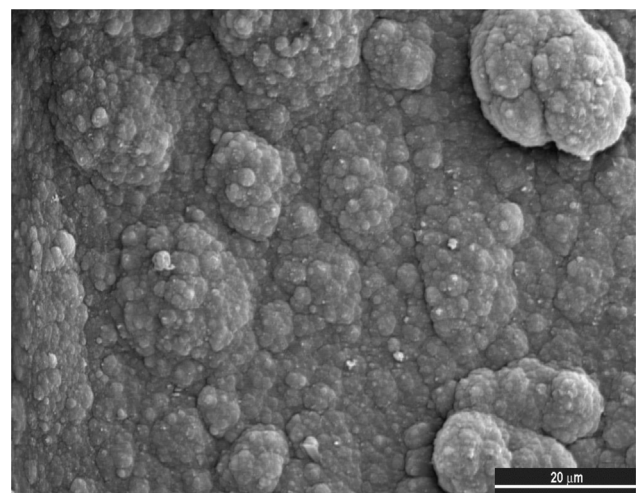


**Fig. 8.** SEM micrograph at different magnifications of SAE/PPy-Zn(20 °C) after 30 days of immersion in 0.5 M NaCl.

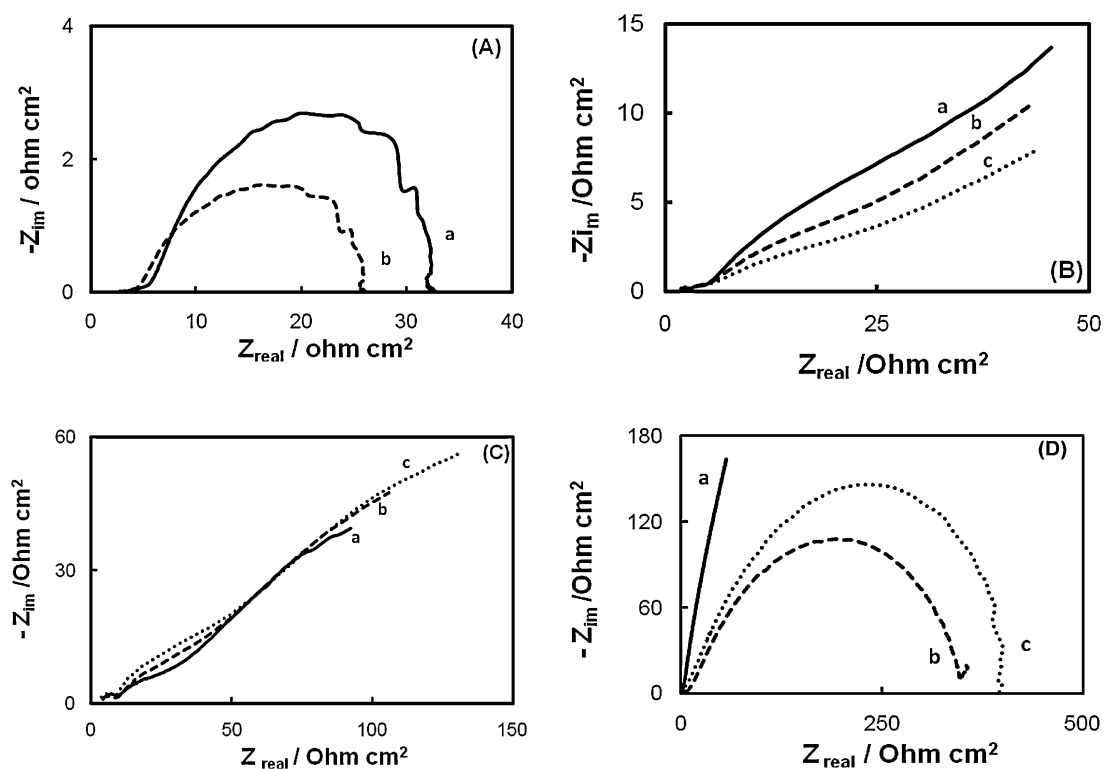


**Fig. 9.** Nyquist plots of the impedance spectra for the samples at the open circuit potential in 0.5 M NaCl after different immersion times: (A) uncoated SAE 4140 steel: (a) 5 min and (b) 90 min; (B) PPy(20°C): (a) 5 min, (b) 180 min and (c) 360 min; (C) PPy-Zn(20°C): (a) 5 min, (b) 15 days and (c) 30 days and (D) PPy-Zn(40°C): (a) 5 min, (b) 15 days and (c) 30 days.

rate that Zn and AOT are incorporated in the polymer matrix during the electrosynthesis.

The Nyquist plot of the bare steel obtained at the open circuit potential exhibits a depressed semicircle according to what it was reported in the literature [18] (Fig. 9A). The response changes significantly when the steel is covered by the coatings. The diagrams obtained for PPy(20°C) and PPy-Zn(20°C) show a rather complex response with three time constants (Fig. 9B and C). Although detailed analysis of the spectra is not attempted here, it can be observed that the magnitude of the total impedance increases with immersion time for PPy-Zn(20°C) while this magnitude decreases in the case of the steel covered with PPy. At the end of the EIS measurements the potential of the steel covered with PPy-Zn(20°C) remains more positive than that corresponding to the uncoated substrate while the potential of the steel covered with PPy(20°C) is close to that of the bare electrode. The differences can be attributed to the less porous structure of PPy-Zn(20°C) (Fig. 2). In addition, it was reported that zinc corrosion products plug the pores of the coating contributing to the corrosion protection of the steel [10].

The impedance spectrum of PPy-Zn(40°C) at the beginning of the immersion shows a linear response with a slope angle greater than 45° indicating a diffusion controlled process (Fig. 9D). As exposure time increases the diagram is characterized by a semicircle whose diameter increases with time.

Tafel plots are shown in Fig. 10. The  $E_{\text{corr}}$ , cathodic ( $B_c$ ) and anodic ( $B_a$ ) Tafel slopes and the estimated corrosion current ( $i_{\text{corr}}$ ) are tabulated in Table 3. The  $i_{\text{corr}}$  values measured for the steel covered with PPy and with PPy-Zn(40°C) are an order of magnitude lower than that of the bare steel while the one covered with PPy-Zn(20°C) exhibited a very low corrosion rate, two orders of magnitude lower.

The potentiodynamic curve of the steel in 0.5 M NaCl obtained at 0.001 V s<sup>-1</sup> shows a current increase at -0.57 V related to pitting

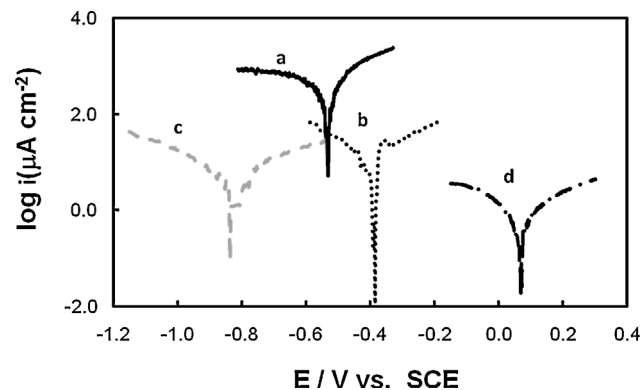


**Fig. 10.** Tafel curves obtained in 0.5 M NaCl for (a) uncoated SAE 4140 steel, (b) PPy(20°C), (c) PPy-Zn(40°C) and (d) PPy-Zn(20°C).

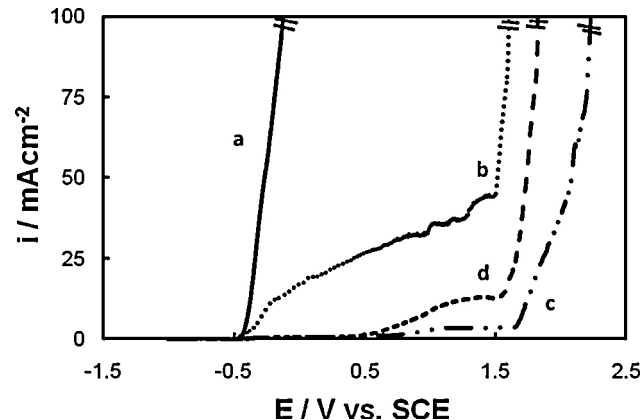


**Fig. 11.** The polarization behavior in 0.5 M NaCl at 0.001 V s<sup>-1</sup> of (a) uncoated SAE 4140 steel, (b) PPy(20°C), (c) PPy-Zn(20°C) and (d) PPy-Zn(40°C).

**Table 3**

Corrosion parameters calculated from Tafel polarization plots for uncoated steel, PPy-coated steel, PPy-Zn(20 °C) coated steel and PPy-Zn(40 °C) coated steel.

Sample	$E_{\text{corr}}$ (V) vs. SCE	$i_{\text{corr}}$ ( $\mu\text{A}/\text{cm}^2$ )	$B_c$ (mV dec $^{-1}$ )	$B_a$ (mV dec $^{-1}$ )
Uncoated SAE 4140 steel	−0.531	74.9	−188	109
SAE/PPy(20 °C)	−0.385	6.3	−210.7	268.8
SAE/PPy-Zn(20 °C)	0.068	0.56	−469.9	268.3
SAE/PPy-Zn(40 °C)	−0.831	3.54	−242.2	202

corrosion (Fig. 11). In the case of the coated samples oxidation and overoxidation of the polymer take place at the more negative potentials. A significant increase in the anodic current occurs only at very positive potentials, being the higher potential for the coating formed at 20 °C. Furthermore, the current increases slowly for the substrate covered with this coating.

The present data show that unmodified PPy electrosynthesized at 20 °C offers some degree of corrosion protection during the early stages, but with continued immersion in chloride solution this protection is lost. It is generally accepted that as a result of the redox process between the polymer and the substrate, the formation of a passive oxide takes place. Furthermore, AOT is a bulky molecule that remains entrapped in the polymer matrix, hindering the ingress of chloride from the electrolyte. The main reason that explains the lost of protection is the open structure of the film that finally allows the electrolyte access (Fig. 6). The corrosion protection properties are significantly improved when Zn is incorporated in the coating because the pores become filled or blocked by its corrosion products [10]. The steel covered with this type of coating formed at 20 °C exhibits a shift to higher OCP and lower corrosion rate during prolonged exposure times in chloride solution. EIS results also confirm that this coating is effective in inhibiting corrosion.

Decreasing the electropolymerization temperature to 5 °C leads to the formation of non-adherent coatings and consequently it provides substantially less protection against corrosion. When the temperature was raised to 40 °C the corrosion protection mechanism is a galvanic coupling process between the deposited Zn and the substrate. In this case Zn is preferentially located near the steel surface.

One of the reasons for the differences between the characteristics of the coatings formed at 20 °C and 40 °C would be a change in the surfactant aggregation state. According to the phase diagram of the binary system AOT/water when the temperature increases, a lamellar phase changes to an isotropic liquid, which has to be interpreted as a solution of spherical micelles with a volume fraction corresponding to the given proportion of AOT in the system [19]. The formation of bilayers or multilayers at the interface of the electrode takes place at concentrations near the critical micelle concentration (cmc) [20]. The working concentration used in this work is above the cmc because the cmc of AOT in water is 2.2 mM and this value is generally reduced with the addition of electrolytes. It was postulated that the monomer is preferentially dissolved in the micellar assembly due to its hydrophobic nature. Then it is possible that the aggregation state of AOT plays an important role in controlling the electrodeposition process of the polymer. The fact that zinc electrodeposition is favored with respect to PPy formation in the absence of AOT confirms that the presence of the surfactant facilitates the electropolymerization process.

On the other hand, the electrodeposition temperature affects the kinetics of polymerization as well as the redox properties and conductivity of PPy films [21,22]. It has been proposed that at higher temperatures the formation of more structural defects due to side reactions such as solvent discharge and nucleophilic attack on polymeric radicals produces lower conductivities of films. Both, PPy films and Zn-modified PPy coatings showed a decrease in the

**Table 4**

Electrical conductivity values obtained for SAE/PPy(20 °C), SAE/PPy(40 °C), SAE/PPy-Zn(20 °C) and SAE/PPy-Zn(40 °C).

Sample	Conductivity ( $\Omega^{-1} \text{cm}^{-1}$ )
SAE/PPy-Zn(20 °C)	$8.9 \times 10^{-2}$
SAE/PPy-Zn(40 °C)	$1.25 \times 10^{-4}$
SAE/PPy(20 °C)	$7.5 \times 10^{-4}$
SAE/PPy(40 °C)	$2.34 \times 10^{-5}$

conductivity when the electrodeposition temperature was increased from 20 °C to 40 °C (Table 4). Considering the influence of the temperature on Zn electrodeposition, the charge involved in this process increased with increasing temperature.

Several studies show that the structure and electrical conductivity of conducting polymers strongly affect their anticorrosive properties [23,24]. It has been demonstrated that an open structure provided less corrosion protection and that these films showed low conductivity values. Moreover, it has been reported that the presence of an anionic surfactant has positive effect on the conductivity of PPy [25,26]. In this work, it was demonstrated that the higher conductivity corresponds to PPy modified at 20 °C which also shows a more compact structure. This result is consistent with the anticorrosive performance of the coatings.

#### 4. Conclusions

A simple one-step method for the electrodeposition of PPy films modified with Zn onto SAE 4140 steel was employed. The coatings were obtained by a potentiodynamic technique in a neutral AOT solution containing ZnSO<sub>4</sub> and Py. Zn incorporation improves the anticorrosive performance of PPy films. Zn particles and its corrosion products plug up the polymer pores increasing the barrier properties of the films. The coating with optimum characteristics in terms of anticorrosion properties was obtained at 20 °C.

The combination of PPy and Zn electrodeposited at 40 °C provides a cathodic protection to the substrate. The adherence and anticorrosion properties decrease for the coatings electrosynthesized at 5 °C.

#### Acknowledgements

CONICET, ANPCYT and Universidad Nacional del Sur, Bahía Blanca, Argentina are acknowledged for financial support.

#### References

- [1] J.W. Schultze, H. Karabulut, *Electrochim. Acta* 50 (2005) 1739–1745.
- [2] M. Rohwerder, A. Michalik, *Electrochim. Acta* 53 (2007) 1300–1313.
- [3] S. Bialozor, A. Kupniewska, *Synth. Met.* 155 (2005) 443–449.
- [4] G. Inzelt, M. Pineri, J.W. Schultze, M.A. Vorotynets, *Electrochim. Acta* 45 (2000) 2403–2421.
- [5] M.A. Malik, M.T. Galkowski, H. Bala, B. Grzybowska, P.J. Kulesza, *Electrochim. Acta* 44 (1999) 2157–2163.
- [6] E. Armelin, M. Marti, F. Liesa, J.I. Iribarren, C. Aleman, *Prog. Org. Coat.* 69 (2010) 26–30.
- [7] E. Akbarinezhad, M. Ebrahimi, F. Sharif, M.M. Attar, H.R. Faridi, *Prog. Org. Coat.* 70 (2011) 39–44.

- [8] N. Boshkov, N. Tsvetkova, P. Petrov, D. Koleva, K. Petrov, G. Avdeev, Ch. Tsvetanov, G. Raichevsky, R. Raicheffe, *Appl. Surf. Sci.* 254 (2008) 5618–5625.
- [9] A. Olad, M. Barati, S. Behboudi, *Prog. Org. Coat.* 74 (2012) 221–227.
- [10] T. Tüken, *Surf. Coat. Technol.* 201 (2006) 2782–2790.
- [11] T. Tüken, B. Yazici, M. Erbil, *Mater. Chem. Phys.* 99 (2006) 459–464.
- [12] P. Herrasti, F.J. Recio, P. Ocón, E. Fatás, *Prog. Org. Coat.* 54 (2005) 285–291.
- [13] I.L. Lehr, S.B. Saidman, *Mater. Chem. Phys.* 10 (2006) 262–267.
- [14] I.L. Lehr, S.B. Saidman, *Corros. Sci.* 49 (2007) 2210–2225.
- [15] D.O. Flamini, S.B. Saidman, *Electrochim. Acta* 55 (2010) 3727–3733.
- [16] I.L. Lehr, S.B. Saidman, *Appl. Surf. Sci.* 258 (2012) 4417–4423.
- [17] G. Zou, W. Chen, R. Liu, Z. Xu, *Mater. Lett.* 61 (2007) 4305–4308.
- [18] T. Tüken, G. Arslan, B. Yazici, M. Erbil, *Corros. Sci.* 46 (2004) 2743–2754.
- [19] P. Petrov, S. Ahir, E. Terentjev, *Langmuir* 18 (2002) 9133–9139.
- [20] U. Retter, M. Tschachnikova, *J. Electroanal. Chem.* 550/551 (2003) 201–208.
- [21] S. Sadki, P. Schottland, N. Brodie, G. Sabouraud, *Chem. Soc. Rev.* 29 (2000) 283–293.
- [22] J. Rodriguez, H.J. Grande, T.F. Otero, in: H.S. Nalwa (Ed.), *Handbook of Organic Conductive Molecules and Polymers*, John Wiley & Sons, New York, 1997.
- [23] C.K. Tan, D.J. Blackwood, *Corros. Sci.* 45 (2003) 545–551.
- [24] A. Olad, M. Barati, H. Shirmohammadi, *Prog. Org. Coat.* 72 (2011) 599–604.
- [25] J. Stejskal, M. Omastová, S. Fedorova, J. Prokes, M. Trchová, *Polymer* 44 (2003) 1353–1358.
- [26] Y. Kudoh, *Synth. Met.* 79 (1996) 17–22.